PHYSICAL SCIENCES: Earth, Atmospheric, and Planetary Sciences

Title: Impact of fossil fuel emissions on atmospheric radiocarbon and various applications of radiocarbon over this century

Short title: Impact of fossil fuel emissions on radiocarbon

H. D. Graven[1*]

[1] Department of Physics and Grantham Institute, Imperial College London
South Kensington Campus, London, SW7 2AZ UK

[*]Corresponding author: h.graven@imperial.ac.uk

Keywords: Fossil fuel emissions, radiocarbon, atmospheric CO_2, ^{14}C dating, emissions scenarios, isotope forensics

Abstract:

Radiocarbon analyses are commonly used in a broad range of fields, including earth science, archaeology, forgery detection, isotope forensics, and physiology. Many applications are sensitive to the radiocarbon (^{14}C) content of atmospheric CO_2, which has varied since 1890 as a result of nuclear weapons testing, fossil fuel emissions, and CO_2 cycling between atmospheric, oceanic, and terrestrial carbon reservoirs. Over this century, the ratio $^{14}C/C$ in atmospheric CO_2 ($\Delta^{14}CO_2$) will be determined by the amount of fossil fuel combustion, which decreases $\Delta^{14}CO_2$ because fossil fuels have lost all ^{14}C from radioactive decay. Simulations of $\Delta^{14}CO_2$ using the emission scenarios from the Intergovernmental Panel on Climate Change Fifth Assessment Report, the Representative Concentration Pathways, indicate that ambitious emission reductions could sustain $\Delta^{14}CO_2$ near the preindustrial level of 0‰ through 2100, whereas “business-as-usual” emissions will reduce $\Delta^{14}CO_2$ to −250‰, equivalent to the depletion expected from over 2,000 y of radioactive decay. Given current emissions trends, fossil fuel emission-driven artificial “aging” of the atmosphere is likely to occur much faster and with a larger magnitude than previously expected. This finding has strong and as yet unrecognized implications for many applications of radiocarbon in various fields, and it implies that radiocarbon dating may no longer provide definitive ages for samples up to 2,000 y old.

Significance statement:

A wide array of scientific disciplines and industries use radiocarbon analyses; for example, it is used in dating of archaeological specimens and in forensic identification of human and wildlife tissues, including traded ivory. Over the next century, fossil fuel emissions will produce a large amount of CO_2 with no ^{14}C because fossil fuels have lost all ^{14}C over millions of years of radioactive decay. Atmospheric CO2, and therefore newly produced organic material, will appear as though it has “aged,” or lost ^{14}C by decay. By 2050, fresh organic material could have the same $^{14}C/C$ ratio as samples from 1050, and thus be indistinguishable by radiocarbon dating. Some current applications for ^{14}C may cease to be viable, and other applications will be strongly affected.

Introduction:

Radiocarbon is produced naturally in the atmosphere and decays with a half-life of 5,700 ± 30 y (1–3). Fossil fuels which are millions of years old, are therefore devoid of 14C, and their combustion adds only the stable isotopes 12C and 13C to the atmosphere as CO2. First observed by Hans Suess in 1955 using tree ring records of atmospheric composition (4), the dilution of $^{14}CO_2$ by fossil carbon provided one of the first indications that human activities were strongly affecting the global carbon cycle. The apparent “aging” of the atmosphere—i.e., the decreasing trend in the ratio $^{14}C/C$ of CO_2 (reported as $\Delta^{14}CO_2$) (5)—was interrupted in the 1950s when nuclear weapons testing produced an immense amount of “bomb” ^{14}C that approximately doubled the ^{14}C content of the atmosphere. Direct atmospheric observations began in the 1950s, capturing the rapid rise of $\Delta^{14}CO_2$ and its subsequent quasi-exponential decay as the bomb ^{14}C mixed into oceanic and biospheric reservoirs (6–9) (Fig. 1).

Now that several decades have passed since the Partial Nuclear Test Ban Treaty and the peak in atmospheric $\Delta^{14}CO_2$, fossil fuel emissions are once again the main influence on the long-term trend in $\Delta^{14}CO_2$ (7, 10). The growth or decline of fossil fuel emissions over the coming century determines to what extent $\Delta^{14}CO_2$ will be diluted further by fossil carbon. Also important is how atmospheric $\Delta^{14}CO_2$ dilution is moderated by natural exchanges of CO_2 with the ocean and the terrestrial biosphere. Future dynamics of carbon and ^{14}C are simulated here using the Representative Concentration Pathways (RCPs) developed for the Intergovernmental Panel on Climate Change (IPCC) Fifth Assessment Report (11, 12), and a simple carbon cycle model with parameters constrained by 20th-century atmospheric and oceanic $\Delta^{14}C$ and CO_2 observations (10, 13) (SI Text).

The simple carbon cycle model includes a one-dimensional box diffusion model of the ocean and represents the atmosphere and the biosphere as one-box carbon reservoirs (10, 13, 14). Exchanges of carbon and ^{14}C are governed by a small number of model parameters (Table S1).Multiple simulations were run using various parameter sets selected by their representation of $\Delta^{14}C$ and inventories of CO_2 and bomb ^{14}C(15–17). Atmospheric CO_2 concentration and fossil fuel and land use fluxes were prescribed by the RCPs, which include historical data through 2005. To match the prescribed atmospheric CO_2 concentration, the residual of carbon emissions and atmospheric and oceanic accumulation was added to the biospheric reservoir (single deconvolution). Atmospheric $\Delta^{14}CO_2$ was prescribed by observations until 2005, then predicted by model fluxes from 2005 to 2100 (SI Text).

Results:

From its present value of ~20‰ (18), which signifies a 2% enrichment in $^{14}C/C$ of CO_2 above preindustrial levels, $\Delta^{14}CO_2$ is certain to cross below the preindustrial level of 0 ‰ by 2030, but potentially as soon as 2019 (Fig. 1, Table S2). After 2030, simulated $\Delta^{14}CO_2$ trends diverge according to the continued growth, slowing, or reversal of fossil fuel CO_2 emissions in the RCP scenarios. Distinct patterns are simulated for different RCPs despite the range of model parameters used, indicating the fossil fuel emissions scenario is the determining factor for long-term $\Delta^{14}CO_2$ trends in these simulations rather than the rates of carbon cycling.

In the low-emission RCP2.6 simulation where fossil fuel emissions decrease after 2020, $\Delta^{14}CO_2$ remains nearly constant around −15‰ through the end of the century (Fig. 1). Fossil fuel emissions in the RCP4.5 and RCP6.0 scenarios continue to rise and then peak later, around 2040 and 2080, reducing $\Delta^{14}CO_2$ to a level of −80‰ (RCP4.5) or −150‰ (RCP6.0) in 2100.

The business-as-usual emissions in RCP8.5 reduce $\Delta^{14}CO_2$ more rapidly and more dramatically than the other RCPs: $\Delta^{14}CO_2$ is less than −100‰ by 2050 and reaches −250‰ in 2100, which means that atmospheric CO_2 in 2100 is as depleted in ^{14}C as the "oldest" part of the ocean (19) (Fig. 2).

The simulated trends in atmospheric $\Delta^{14}CO_2$ propagate to other carbon reservoirs through natural carbon exchanges (Fig. 2). Reduction of fossil fuel emissions in RCP2.6 leads to nearly steady Δ14C in atmospheric, biospheric, and upper ocean carbon in 2100, slightly elevated above preindustrial levels.

As atmospheric $\Delta^{14}CO_2$ decreases strongly in the higher-emission scenarios, it becomes much more depleted in ^{14}C than actively overturning carbon in the oceanic and biospheric reservoirs (shown for RCP8.5 in Fig. 2). After 2050, the simulated air-sea gradient of $\Delta^{14}C$ in RCP8.5 is −50‰, opposite of the preindustrial gradient, and by 2100 atmospheric $\Delta^{14}CO_2$ is 150‰ lower than $\Delta^{14}C$ at midthermocline depths of 600 m. Reversal of $\Delta^{14}C$ gradients causes natural exchanges to transfer ^{14}C from the ocean to the atmosphere (Fig. S1), as shown by Caldeira et al. (20). Caldeira et al. (20) used a similar carbon cycle model with the IS92-A scenario from the IPCC Third Assessment Report (21), which is comparable to RCP6.0. Emissions over the past 10 y have outpaced the IS92-A and RCP6.0 scenarios, and are currently on track to follow RCP8.5 (22). $\Delta^{14}CO_2$ is nearly 50‰ lower in 2050 and 100‰ lower in 2100 in RCP8.5 compared with RCP6.0 (Fig. 1), suggesting that fossil fuel emissions are likely to reduce $\Delta^{14}CO_2$ much faster than expected from the IS92-A scenario used by Caldeira et al. (20). As a result, the atmospheric inventory of ^{14}C could approach the peak ^{14}C inventory from the early 1960s later this century (Fig. S1).

Discussion

Though these simulations indicate tremendous changes to the global radiocarbon cycle and the use of radiocarbon in earth science and biogeochemical research, the potential impacts of future trends in $\Delta^{14}CO_2$ are much broader. Radiocarbon is currently used in a wide array of scientific and industrial applications, many of which exploit its radioactive decay to determine the age of carbon-containing specimens through radiocarbon dating.

Atmospheric CO_2 is presently aging at a rate of ∼30 y·y−1, and by 2050 the atmosphere could appear to be 1,000 y old in conventional radiocarbon age (Fig. 1). In 2100, atmospheric CO_2 in RCP8.5 has the same radiocarbon content as a specimen that has undergone 2,000 y of radioactive decay—i.e., a specimen originating around AD 100. The aging of the atmosphere predicted by these simulations has the potential to severely impact the use of radiocarbon dating. Within the next 85 y, the atmosphere may experience $\Delta^{14}CO_2$ corresponding to conventional ages from within the historical period encompassing the Roman, Medieval and Imperial Eras. For archaeological or other items that are found without sufficient context to rule out a modern origin, radiocarbon dating will give ambiguous results.

Radiocarbon has various applications in isotope forensics (23). Some applications use the presence of elevated $\Delta^{14}C$ in a sample to distinguish its origin to be subsequent to 1950, whereas other applications use the rapid changes in $\Delta^{14}CO_2$ after 1963 (the so-called “bomb curve”) to distinguish the year of origin of a sample more precisely. These techniques have been used to test vintages of wine and whisky, identify the age of human remains, and detect illegal ivory trading (23–25). As with radiocarbon dating, forthcoming $\Delta^{14}CO_2$ changes are likely to introduce ambiguity into these techniques, and the presence of elevated $\Delta^{14}CO_2$ will not identify samples with recent origins beyond ~2030.

If the lower-emission RCPs 2.6 or 4.5 were followed instead of business-as-usual RCP8.5, the simulated stabilization of $\Delta^{14}CO_2$ (Fig. 1) would hinder the use of radiocarbon in fields such as ecology and physiology. These applications take advantage of the decreasing trend in $\Delta^{14}CO_2$ since the 1960s to evaluate the decadal-scale rate of turnover of carbon in soil compounds (26) or human cells (27), for example. Annual changes in $\Delta^{14}CO_2$ could become undetectable in two to three decades if CO_2 emissions are rapidly reduced, thereby limiting the use of these applications.

Another prominent application for radiocarbon involves the identification of CO_2 emitted by fossil fuel combustion in urban or continental regions (28, 29). Here too, the projected atmospheric changes will have a major impact. The sensitivity of $\Delta^{14}CO_2$ to local additions of fossil fuel-derived CO_2 depends on the concentration of atmospheric CO_2 and the $\Delta^{14}C$ disequilibrium between atmospheric CO_2 and fossil carbon (being ^{14}C-free, the $\Delta^{14}C$ of fossil fuels is −1,000‰). Neglecting other effects, the sensitivity of $\Delta^{14}CO_2$ to fossil fuel-derived CO_2 is approximated by $\alpha \sim (-1{,}000‰ - \Delta^{14}CO_2)/CO_2$. The ratio α is presently −2.6‰ ppm^{-1}, but it drops to −1.6‰ ppm^{-1} by 2050 and to −0.8‰ ppm^{-1} by 2100 in RCP8.5; this suggests that measurement precision will have to increase by approximately a factor of 2 in the next few decades simply to maintain current detection capabilities for fossil fuel-derived CO_2.

Simulated trends in $\Delta^{14}CO_2$ therefore motivate new efforts to improve precision in radiocarbon measurements and to develop ancillary measurements that can help resolve ambiguity in radiocarbon analyses. The development of accelerator mass spectrometry (AMS) in the 1980s dramatically reduced the amount of time and the amount of carbon needed for analysis, compared with traditional decay counting techniques (30, 31). Further improvement in the precision of ^{14}C detection by AMS is needed, as well as reductions in other sources of uncertainty (32), which may change as atmospheric $\Delta^{14}CO_2$ decreases. Ever-higher requirements in precision will also need to be met by alternative measurement techniques currently in development (33).

Fossil fuel emissions are now increasing faster than ever before. Continued business-as-usual growth in emissions will cause the atmosphere to approach a 1,000-y-old radiocarbon age by 2050 and a 2,000-y-old age by 2100. The application of radiocarbon in a wide array of disciplines implies that changing atmospheric radiocarbon content will have far-reaching impacts.

Acknowledgments:

The author thanks S. Frolking, P. Reimer, E. Kato, and T. Guilderson for helpful discussions and the RCP Task Group for providing CO_2 concentration and emission scenarios, and acknowledges support from the European Commission through a Marie Curie Career Integration Grant.

References

1. Godwin H (1962) Half-life of radiocarbon. *Nature* 195:984.

2. Libby WF, Anderson EC, Arnold JR (1949) Age determination by radiocarbon content: World-wide assay of natural radiocarbon. *Science* 109(2827):227–228.

3. Roberts ML, Southon JR (2007) A preliminary determination of the absolute $^{14}C/^{12}C$ ratio of OX-I. *Radiocarbon* 49(2):441–445.

4. Suess HE (1955) Radiocarbon concentration in modern wood. *Science* 122(3166): 415–417.

5. Stuiver M, Polach HA (1977) Discussion: Reporting of ^{14}C data. *Radiocarbon* 19(3): 355–363.

6. Rafter TA, Fergusson GJ (1957) “Atom bomb effect”—Recent increase of carbon-14 content of the atmosphere and biosphere. *Science* 126(3273):557–558.

7. Levin I, et al. (2010) Observations and modelling of the global distribution and longterm trend of atmospheric $^{14}CO_2$. *Tellus B Chem Phys Meterol* 62(1):26–46.

8. Manning MR, et al. (1990) The use of radiocarbon measurements in atmospheric studies. *Radiocarbon* 32(1):37–58.

9. Nydal R, Lövseth K (1983) Tracing bomb 14C in the atmosphere. *J Geophys Res* 88(C6): 3621–3642.

10. Graven HD, Guilderson TP, Keeling RF (2012) Observations of radiocarbon in CO2 at La Jolla, California, USA 1992-2007: Analysis of the long-term trend. *J Geophys Res Atmos* 117(D2):D02302.

11. van Vuuren DP, et al. (2011) The representative concentration pathways: An overview. *Clim Change* 109(1-2):5–31.

12. Intergovernmental Panel on Climate Change (2013) Climate Change 2013: The Physical Science Basis. Contribution of Working Group I to the Fifth Assessment Report of the Intergovernmental Panel on Climate Change, eds Stocker TF, et al (Cambridge Univ Press, Cambridge, UK).

13. Oeschger H, Siegenthaler U, Schotterer U, Gugelmann A (1975) A box diffusion model to study the carbon dioxide exchange in nature. *Tellus* 27(2):168–192.

14. Keeling CD, et al. (1989) A three-dimensional model of atmospheric CO_2 transport based on observed winds: 1. Analysis of observational data. Aspects of Climate Variability in the Pacific and the Western Americas, ed Peterson DH (American Geophysical Union, Washington, DC), pp 165–236.

15. Naegler T, Levin I (2006) Closing the global radiocarbon budget 1945–2005. *J Geophys Res* 111(D12).

16. Naegler T (2009) Reconciliation of excess ^{14}C-constrained global CO_2 piston velocity estimates. *Tellus B Chem Phys Meterol* 61(2):372–384.

17. Sabine CL, et al. (2004) The oceanic sink for anthropogenic CO_2. *Science* 305(5682): 367–371.

18. Levin I, Kromer B, Hammer S (2013) Atmospheric $\Delta^{14}CO_2$ trend in Western European background air from 2000 to 2012. *Tellus B Chem Phys Meterol* 65:20092.

19. Key RM, et al. (2004) A global ocean carbon climatology: Results from Global Data Analysis Project (GLODAP). *Global Biogeochem Cycles*, 10.1029/2004GB002247.

20. Caldeira K, Rau GH, Duffy PB (1998) Predicted net efflux of radiocarbon from the ocean and increase in atmospheric radiocarbon content. *Geophys Res Lett* 25(20): 3811–3814.

21. Leggett J, Pepper WJ, Swart RJ (1992) Emissions Scenarios for IPCC: An update. Climate Change 1992. The Supplementary Report to the IPCC Scientific Assessment, eds Houghton JT, Callander BA, Varney SK (Cambridge Univ Press, Cambridge, UK).

22. Peters GP, et al. (2012) The challenge to keep global warming below 2°C. *Nature Climate Change* 3(1):4–6.

23. Geyh MA (2001) Bomb radiocarbon dating of animal tissues and hair. *Radiocarbon* 43(2B):723–730.

24. Uno KT, et al. (2013) Bomb-curve radiocarbon measurement of recent biologic tissues and applications to wildlife forensics and stable isotope (paleo)ecology. *Proc Natl Acad Sci USA* 110(29):11736–11741.

25. Ubelaker DH (2001) Artificial radiocarbon as an indicator of recent origin of organic remains in forensic cases. *J Forensic Sci* 46(6):1285–1287.

26. Trumbore SE (2000) Age of soil organic matter and soil respiration: Radiocarbon constraints on belowground C dynamics. *Ecol Appl* 10(2):399–411.

27. Spalding KL, Bhardwaj RD, Buchholz BA, Druid H, Frisén J (2005) Retrospective birth dating of cells in humans. *Cell* 122(1):133–143.

28. Levin I, Kromer B, Schmidt M, Sartorius H (2003) A novel approach for independent budgeting of fossil fuel CO_2 over Europe by $^{14}CO_2$ observations. *Geophys Res Lett*, 10.1029/2003GL018477.

29. Turnbull JC, et al. (2006) Comparison of $^{14}CO_2$, CO, and SF_6 as tracers for recently added fossil fuel CO_2 in the atmosphere and implications for biological CO_2 exchange. *Geophys Res Lett*, 10.1029/2005GL024213.

30. Vogel JS, Turteltaub KW, Finkel R, Nelson DE (1995) Accelerator mass spectrometry. *Anal Chem* 67(11):353A–359A.

31. Elmore D, Phillips FM (1987) Accelerator mass spectrometry for measurement of longlived radioisotopes. *Science* 236(4801):543–550.

32. Graven HD, Guilderson TP, Keeling RF (2007) Methods for high-precision ^{14}C AMS measurement of atmospheric CO_2 at LLNL. *Radiocarbon* 49(2):349–356.

33. Galli I, et al. (2011) Molecular gas sensing below parts per trillion: Radiocarbondioxide optical detection. *Phys Rev Lett* 107(27):270802.

34. Meinshausen M, et al. (2011) The RCP greenhouse gas concentrations and their extensions from 1765 to 2300. *Clim Change* 109(1-2):213–241.

35. Graven HD, Guilderson TP, Keeling RF (2012) Observations of radiocarbon in CO_2 at seven global sampling sites in the Scripps flask network: Analysis of spatial gradients and seasonal cycles. *J Geophys Res Atmos* 117(D2):D02303.

36. Stuiver M, Reimer PJ, Braziunas TF (1998) High-precision radiocarbon age calibration for terrestrial and marine samples. *Radiocarbon* 40(3):1127–1151.

37. Graven HD, Gruber N (2011) Continental-scale enrichment of atmospheric $^{14}CO_2$ from the nuclear power industry: Potential impact on the estimation of fossil fuel-derived CO_2. *Atmos Chem Phys* 11:12339–12349.

38. Peng TH, Takahashi T, Broecker WS, Olafsson JON (1987) Seasonal variability of carbon dioxide, nutrients and oxygen in the northern North Atlantic surface water: Observations and a model*. *Tellus B Chem Phys Meterol* 39(5):439–458.

Figure legends:

Fig. 1. Model predictions of atmospheric radiocarbon for the RCPs. (Left) Atmospheric CO_2 concentration (Top), CO_2 emissions from fossil fuel combustion (Middle), and CO_2 emissions from land use change (Bottom) in the RCP scenarios (11, 34). (Middle) Fossil fuel CO_2 emitted to the atmosphere is shown with solid lines; dashed lines show net fossil fuel CO_2 emitted, including "negative emissions" from biomass energy with carbon capture and storage. (Right) Observed (7, 10, 18, 35, 36) (1940–2012) and projected (2005–2100) radiocarbon content of atmospheric CO_2 ($\Delta^{14}CO_2$) (Table S2). The right axis shows the conventional radiocarbon age of a carbon-containing specimen with the same radiocarbon content, calculated by $8033 * \ln(\Delta^{14}C/1{,}000 + 1)$. Filled areas indicate the range simulated for different sets of model parameters, each consistent with 20th-century atmospheric and oceanic $\Delta^{14}C$ and CO_2 observations, within their uncertainties (10) (SI Text).

Fig. 2. Simulation of radiocarbon in various carbon reservoirs for the low-emission and business-as-usual RCPs. Simulated $\Delta^{14}C$ in biospheric and four ocean carbon reservoirs, surface mixed layer, 300, 600, and 3,500 m in RCP2.6 (Left) and RCP8.5 (Right). The black line shows the midrange value of simulated atmospheric $\Delta^{14}CO_2$ (full simulated range of $\Delta^{14}CO_2$ is shown in Fig. 1).

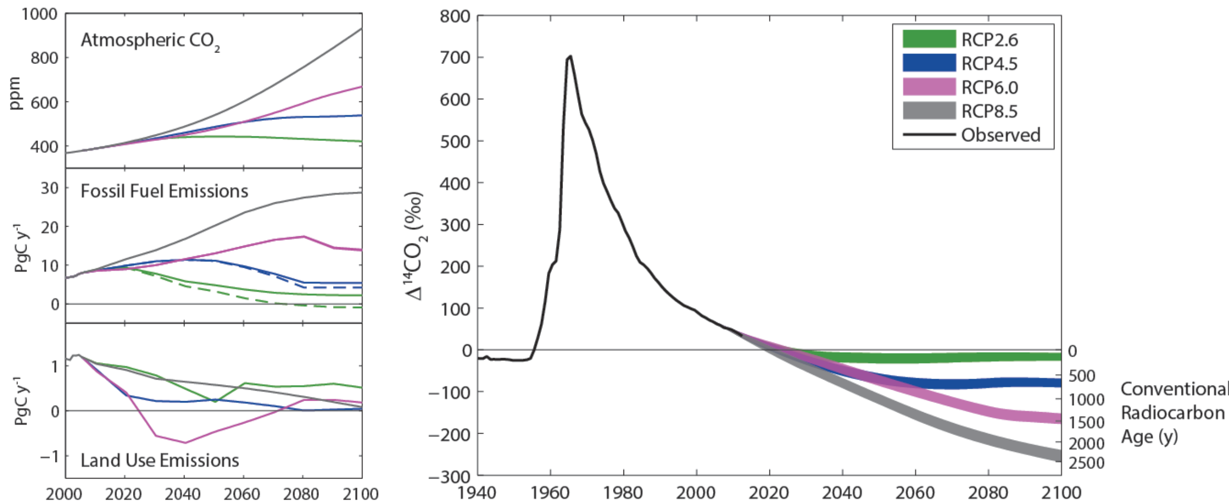

Atmospheric CO_2
ppm
Fossil Fuel Emissions
PgC y[-1]
Land Use Emissions
PgC y[-1]
RCP2.6
RCP4.5
RCP6.0
RCP8.5
Observed
Δ[14]CO_2 (‰)
Conventional
Radiocarbon
Age (y)

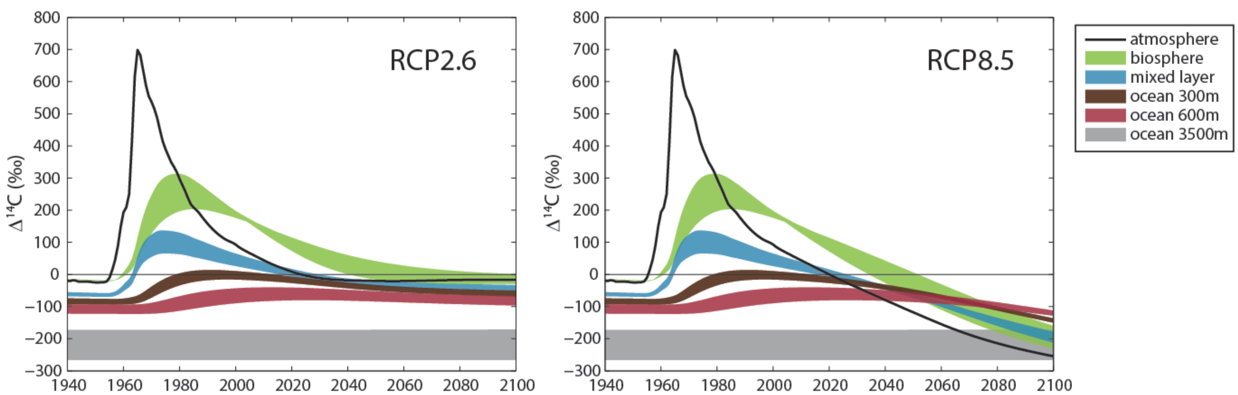

RCP2.6
RCP8.5
Δ[14]C (‰)
atmosphere
biosphere
mixed layer
ocean 300m
ocean 600m
ocean 3500m